

Diffusion of Gold and Silver in Bisphenol A Polycarbonate

Ralf Willecke*[†] and Franz Faupel*Lehrstuhl für Materialverbunde, Technische Fakultät der Universität Kiel, Kaiserstrasse 2, 24143 Kiel, Germany**Received September 27, 1995; Revised Manuscript Received October 3, 1996*[®]

ABSTRACT: Diffusion of evaporated gold and silver into Bisphenol A polycarbonate has been studied using the radiotracer technique in combination with ion beam sputtering for serial sectioning. Diffusion coefficients between 4×10^{-14} and 1×10^{-16} cm² s⁻¹ were measured in the temperature range between 210 and 130 °C. The metal concentration in the polymer turned out to depend strongly on the evaporation rate. An Arrhenius-like temperature dependence with activation energies of 1.02 eV for silver and 1.13 eV for gold was found. The low diffusivities, which are not affected by the polymer dynamics, are interpreted within molecular theories for diffusion of gases in polymers with an additional attractive interaction between metal atoms and polymer chains.

1. Introduction

While diffusion of gases and organic molecules in polymers has been the subject of many investigations,^{1–3} knowledge of metal diffusion in polymers is very limited. Transport of metal ions in solid polymer electrolytes is understood best.^{4,5} It was investigated by conductivity and direct radiotracer measurements. The mobility of ions in polymer electrolytes is comparable with the mobility of ions in liquid electrolytes. Arrhenius plots exhibit a downward curvature which has been interpreted in terms of coupling of the movement of the ions and the segments of the polymer chains.^{4,5} Metal ions can be incorporated into polymer electrolytes like poly(ethylene oxide) (PEO) because these are able to dissolve the corresponding metal salt. Alkali and other metals that reduce polymers can be introduced directly.^{6–8}

Recently, diffusion of neutral gold clusters, which have been used as inert markers in polymer interdiffusion measurements, has been observed at elevated temperatures above the glass transition.^{9,10} Here diffusion can be interpreted as Brownian movement of the metal particles in a viscous liquid.¹¹

Investigations of metal diffusion at lower temperatures near or below the glass transition of the polymer were stimulated by applications of metal–polymer structures in every day use and high-tech application for instance in microelectronics.^{12–15} Investigations with X-ray photoemission spectroscopy (XPS) were carried out to characterize the chemical interaction of metals with the polymer.^{16,17} In these experiments the intensity of the copper signal decreased, when copper was evaporated onto polyimide at nominal copper coverages below one monolayer and held at elevated temperatures for several hours. This behavior was attributed to diffusion of single copper atoms into the polymer.

Several investigations have been carried out, using Rutherford back-scattering (RBS)^{18,19} and the related technique of medium energy ion scattering (MEIS),²⁰ to determine the diffusion behavior of metals in polyimides. Cu and Ag were found to diffuse into polyimides at elevated temperatures. For more reactive metals such as Mo¹⁹ and the reactive Cr²¹ no diffusion could be detected.

Direct radiotracer experiments in combination with the ion beam sputtering for serial sectioning have been performed to measure diffusion of Cu in PMDA–ODA polyimide.^{22,23} Diffusion coefficients of 2×10^{-14} cm² s⁻¹ at 400 °C down to 8×10^{-16} cm² s⁻¹ at 200 °C were measured. The Arrhenius plot showed a downward curvature. A similar downward curvature was found for diffusion of Ag in this polymer^{24,25} below the glass transition temperature of about 400 °C and was interpreted within the free volume theory of Vrentas and Duda.^{26,27} This theory is based on a model of Cohen and Turnbull²⁸ and was developed for temperatures above and below the glass transition. The evaluation in terms of the free volume theory suggests very low coupling of metal diffusion to the segment mobility of the polymer chains.²⁴

A downward curvature in the Arrhenius plot has frequently been observed for diffusion of larger molecules with diffusion coefficients of 10^{-12} to 10^{-14} cm² s⁻¹ at T_g in polymers above the glass transition temperature.^{1,29} This behavior and a change of the effective activation energy at the glass transition can be well explained by the free volume theory. On the other hand the diffusion of small molecules of gases and simple solvents, which have much higher diffusion coefficients in the range of 10^{-8} cm² s⁻¹, usually shows an Arrhenius-like temperature dependence.^{1–3} Here diffusion is normally not affected by the glass transition. In this light it is surprising that noble metal atoms with a size comparable to small gas molecules are much less mobile in polymers, while the features of their diffusion behavior can be understood in terms of the free volume theory. This points to a substantial metal–polymer interaction, which can be incorporated into the preexponential factor of free-volume theories.^{26,27}

Unfortunately, data of metal diffusion in polymers are very rare and only restricted to the technologically important polyimides. These polymers provide a very limited temperature range above the glass transition, because the decomposition temperature is only slightly higher than the glass transition temperature.¹² Therefore, a systematic investigation of diffusion is not possible in the rubbery state.

In the present work the amorphous polymer Bisphenol A polycarbonate (BPA) was chosen in order to compare metal diffusion with diffusion of larger molecules or gases and to clarify the mechanism of metal diffusion in polymers. For Bisphenol A polycarbonate many data on diffusion and the polymer dynamics are

[†] Temporary address: Materials Laboratory for Interconnect and Packaging, University of Texas at Austin, Austin, TX 78712-1100.

[®] Abstract published in *Advance ACS Abstracts*, January 1, 1997.

available.^{29–32} Because of the glass temperature of 150 °C measurements of metal diffusion are possible over a wide temperature range above T_g . Arrhenius plots for diffusion of large molecules in BPA show a downward curvature and a change in the apparent activation energy at the glass transition, which has been interpreted in terms of the free volume theory.²⁹ Gases, on the other hand, follow an Arrhenius-like behavior in this polymer.³²

2. Experimental Procedure

Bisphenol-A polycarbonate ($M_n = 14200$; $M_w = 29300$), which was kindly provided by Bayer AG, Leverkusen, Germany, was available as sheets of 2 mm thickness. Small pieces of the polymer were cut off and were dissolved in dichloromethane in a 10 wt % viscous solution. The solution was cast onto a clean silicon wafer of 0.5 mm thickness and subsequently poured off. Thus, a film of about 3 μm thickness remained on the wafer and a smooth surface was obtained. Small samples of about $15 \times 15 \text{ mm}^2$ in size were cut from this wafer.

The radioactive tracers $^{110\text{m}}\text{Ag}$ and ^{198}Au were produced by neutron activation of small metallic pieces of about 0.5 mg of Ag for 5 weeks or 0.1 mg of Au for 2 days with a neutron flux of 5×10^{13} neutrons/s. The isotope $^{110\text{m}}\text{Ag}$ decays with a lifetime of 250 days by β^- decay under emission of 658, 764, and 885 keV γ quanta. After activation a specific activity of 1×10^7 Bq/mg was obtained. ^{198}Au , which has a lifetime of 2.7 days and decays under emission of β^- radiation and a 412 keV γ quantum, was produced with a specific activity of about 5×10^8 Bq/mg.

The diffusion annealing was carried out under high vacuum better than 10^{-3} Pa. The samples were mounted on a copper plate with heat-conducting paste and covered with a 10 mm aperture. The plate was heated with a resistance heater, and the temperature was measured with a Ni/NiCr thermocouple and kept constant within ± 0.5 K with a temperature controller (Eurotherm 92). The sample was held at the annealing temperature for at least 10 min before the radioactive tracer was evaporated onto the hot sample. For annealing temperatures below 170 °C (20 K above the glass transition) the sample was kept at this temperature for at least 10 min and subsequently slowly cooled to the annealing temperature in order to improve smoothness and to obtain a nearly fully relaxed state. No evidence of residual solvent from the preparation process could be found in the polymer films during this heat treatment under high vacuum. The tracer was evaporated onto the sample from a Knudsen cell with a slow rate below 0.1 monolayer (ML)/min for gold and 0.5 ML/min for silver. This resulted in evaporation times of several minutes which was always less than a quarter of the total annealing time. After annealing, the vacuum chamber with N_2 was immediately vented, to enhance cooling, and the sample was removed.

Serial sectioning was performed under high vacuum using the ion beam sputtering technique.³³ The ion beam was produced by means of an ion source of the Kaufman-type³⁴ (ION TECH). This source allows us to quasi neutralize the ion beam by an electron-emitting filament. Thus, it is possible to avoid charging effects when insulators are sputtered. An accelerator voltage of 150 V (200 V for the highest penetration depths) was used. Thus, high sputter rates of typically 1 nm/min and a good depth resolution of the order of the surface roughness of about 4 nm could be obtained. The sample was mounted on a water-cooled specimen holder, which rotated slowly to obtain a uniform removal of material. An angle of 60° between the ion beam and the surface normal was chosen to achieve a high sputter rate and to minimize surface roughening. The sputtered-off material was collected on a Mylar foil which was advanced in a motor driven camera. Thus, the film could be stepwisely transported, and up to 20 and more sections could be collected. After sectioning, the film was cut into pieces corresponding to the individual sections, and the activity of each section was measured in a well-type

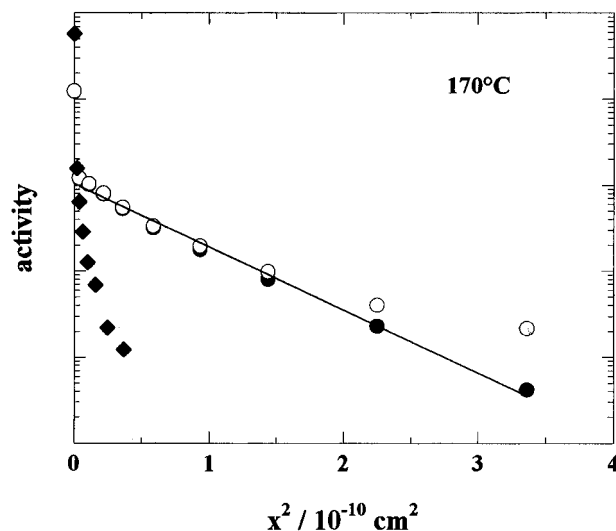


Figure 1. Penetration profile of ^{198}Au into Bisphenol A polycarbonate after annealing at 170 °C for 5800 s. The solid circles represent the original profile (open circles) after correction for the sputter background. A profile of a sample that was not annealed is displayed for comparison (solid diamonds). It represents the resolution function of the present ion-beam sectioning technique.

NaI scintillation counter. The depth of each section was determined from the sputter time and the total depth after the sputter process. This depth was measured by means of a profilometer at an edge between an eroded and a noneroded part of the sample which was covered outside the active evaporation area by a small Mylar strip during sputtering.

3. Results

For the evaluation of the diffusion coefficient the logarithm of activity was plotted versus the square of penetration depth, as shown in Figure 1. This plot implies that the thin-film solution (1) of Fick's second law,

$$c(x, t) = \frac{C}{\sqrt{\pi Dt}} \exp\left(-\frac{x^2}{4Dt}\right) \quad (1)$$

which is valid for the deposition of a thin tracer film at the beginning of the diffusion annealing, can be applied.³⁵ Here C is the number of atoms per unit area. The diffusion coefficient D can be determined from the slope, s , of the linear part of the plot and the diffusion time t : $D = 1/(4st)$. It should be pointed out that the determination of diffusion coefficients from penetration profiles is much more direct than permeation or sorption experiments which are often employed to measure diffusion of gases and organic solvents in polymers. For instance, contributions of a second diffusion mechanism or any x -dependence of the diffusivity would lead to a deviation from linearity in the diffusion profiles and can hence be detected.

Figure 1 shows the penetration profile of ^{198}Au in Bisphenol A polycarbonate at 170 °C. A surface holdup of about one decade is visible, followed by a linear range. At lower concentrations a deviation from linearity (open circles) is caused by spread activity. Radioactive material is sputtered off from the sample, and a small fraction is not collected on the catcher foil but is distributed in the vacuum chamber. After a time lag some of this activity is also sputtered off to the catcher foil and causes background activity. A correction of the activity for this sputter background³³ leads to a penetration profile with a linear range of more than two

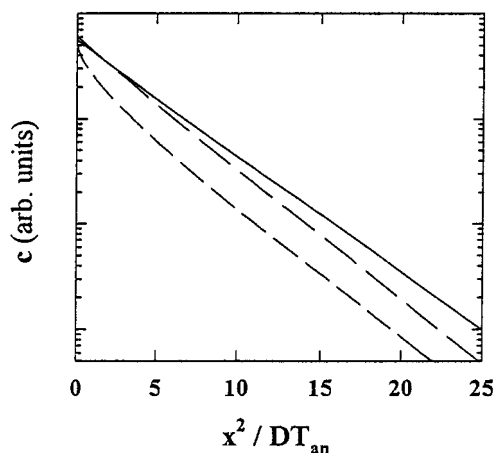


Figure 2. Calculated tracer concentration distributions for different boundary conditions plotted versus the square of the normalized penetration depth x^2/DT_{an} , where T_{an} is the total annealing time. The lines, from top to bottom, represent the thin-film solution of eq 1, the solution given by eq 2 for evaporation of the tracer in the first quarter of the total annealing time, and the solution for solubility limited diffusion according to eq 3.

decades. The third profile in Figure 1 shows the penetration profile of a nonannealed sample and essentially represents the resolution of the sectioning technique by sputtering. It is also broadened by the surface roughness. The broadening of the penetration profiles by surface roughness and final depth resolution could be neglected in the evaluation of diffusion coefficients within experimental error margins.

The strong surface holdup, which is also seen in Figures 3 and 4, appears to be typical of metal diffusion in polymers^{22–25} and can be attributed to the formation of immobile metal clusters at the surface during metal deposition (see Discussion). Under these conditions the applicability of the thin-film solution equation (1) is not obvious. Moreover, the effect of the final evaporation time must be quantified. For an evaporation time T_{ev} at the beginning of the diffusion annealing at a constant rate eq 1 has to be replaced by

$$c(x,t) = \frac{C}{T_{ev}\sqrt{\pi D}} \int_0^{T_{ev}} \frac{1}{\sqrt{t-\tau}} \exp\left(-\frac{x^2}{4D(t-\tau)}\right) d\tau \quad (2)$$

An estimate of the influence of metal aggregation at the surface on the evaluation of the diffusion profiles can be obtained by considering the case of solubility-limited diffusion. Here the concentration distribution is described by the complementary error function³⁵

$$c(x,t) = c_0 \operatorname{erfc}\left(\frac{x}{2\sqrt{Dt}}\right) = c_0 \left[1 - \frac{2}{\sqrt{\pi}} \int_0^{x/2\sqrt{Dt}} e^{-u^2} du\right] \quad (3)$$

where c_0 is the constant surface concentration given by the solubility limit.

Figure 2 shows profiles calculated numerically from eqs 1–3 with the same diffusion coefficient and annealing time. For eq 2 evaporation during the first quarter of the total annealing time with a constant rate was assumed. All three profiles are linear except for the near-surface region, and the slopes, which reflect the diffusivity in the plot of the logarithm of the concentration versus the square of the depth, differ only weakly. Quantitatively, it is found that the diffusion coefficient can be calculated from the thin-film solution if an

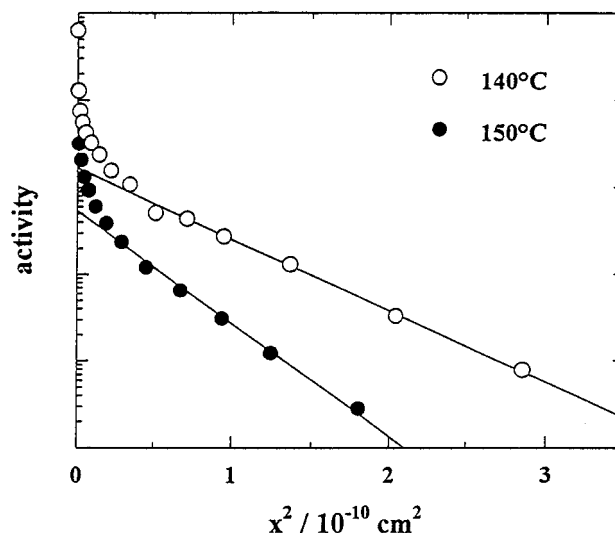


Figure 3. Penetration profiles for diffusion of ^{198}Au into Bisphenol A polycarbonate.

effective annealing time T_{an}^{eff} is used. The difference between the actual annealing time T_{an} and T_{an}^{eff} is small for both eqs 2 and 3. For evaporation of the tracer at a constant rate, T_{an}^{eff} can be very well approximated by $T_{an}^{\text{eff}} = T_{an} - 0.43 T_{ev}$, if the evaporation time T_{ev} does not exceed $T_{an}/4$. For solubility-limited diffusion T_{an}^{eff} is given by $T_{an}^{\text{eff}} = 0.89 T_{an}$. Neither eq 2 nor eq 3 describe the actual diffusion behavior exactly. They do not take into account the effect of trapping of metal atoms in the cluster region near the surface on the slope of the low-concentration tail at larger penetration depth. Computer simulations³⁶ have shown that this trapping may cause an overestimation of the diffusivity, determined from the linear tails of the profiles, by less than 30% under the present experimental conditions.

In the evaluation of the thin-film solution with the effective annealing time, eq 2 was used. The errors introduced by this approximation are less than errors caused by uncertainties in determining the sputter depth, which can be estimated as 20%, and in the slope of the linear range of the penetration plot. Considering an additional small error due to the cooling process, the upper limit for the error in the diffusion coefficient is 50%.

Figures 3 and 4 each show two more profiles with a large linear range for diffusion of Ag and Au, respectively. It is remarkable that for silver the surface holdup is higher by more than a factor of 10 than for gold. The temperatures, diffusion coefficients, and annealing times for all samples are listed in Table 1.

Figure 5 shows the temperature dependence of the diffusion coefficients of silver and gold in an Arrhenius plot where the diffusion coefficients are plotted on a logarithmic scale versus the inverse absolute temperature. The data are well described by an Arrhenius law with the following parameters:

$$D^{\text{Au}}(T) = 2.2 \times 10^{-2} \exp\left(-\frac{1.13 \text{ eV}}{kT}\right) \frac{\text{cm}^2}{\text{s}} \quad (4)$$

$$D^{\text{Ag}}(T) = 1.6 \times 10^{-3} \exp\left(-\frac{1.02 \text{ eV}}{kT}\right) \frac{\text{cm}^2}{\text{s}} \quad (5)$$

The errors in the activation energies are about ± 0.15 eV. The D_0 values give the order of magnitude. Since it is known that BPA polycarbonate may crystallize

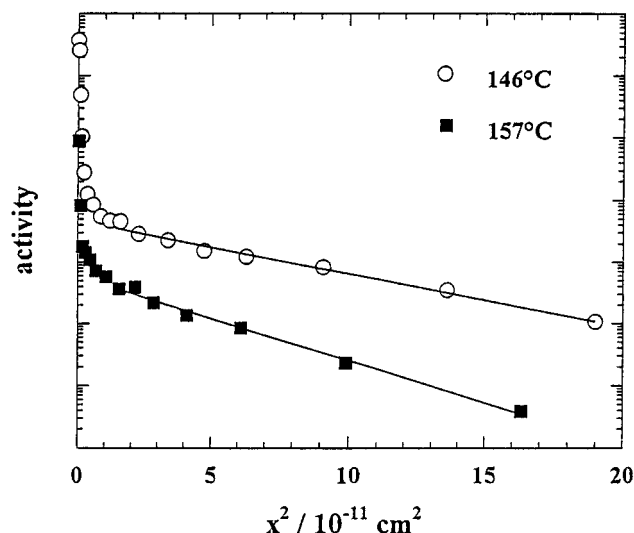


Figure 4. Diffusion profiles for diffusion of ^{110m}Ag into Bisphenol A polycarbonate.

Table 1. Temperatures, Annealing Times, and Diffusion Coefficients for ^{198}Au and ^{110m}Ag Diffusion in Bisphenol A Polycarbonate

tracer	T (K)	t_{eff} (s)	D ($\text{cm}^2 \text{s}^{-1}$)
^{110m}Ag	483	1476	3.4×10^{-14}
	473	1371	3.1×10^{-14}
	453	2013	6.8×10^{-15}
	448	7242	5.2×10^{-15}
	436	2313	2.9×10^{-15}
	430	4242	1.9×10^{-15}
	419	16425	8.0×10^{-16}
	413	12213	7.3×10^{-16}
^{198}Au	483	1320	3.5×10^{-14}
	468	1320	1.4×10^{-14}
	453	1671	5.6×10^{-15}
	443	5800	2.6×10^{-15}
	423	8484	8.2×10^{-16}
	413	41013	3.3×10^{-16}
	403	37284	1.5×10^{-16}

under extreme conditions, we note that the linear Arrhenius law over more than two decades clearly allows one to exclude significant crystallization of samples at the highest temperatures.

4. Discussion

While diffusion and permeation of gases and solvents in polymers^{31,32} involve ordinary solution, the extent of metal diffusion into polymers depends on the deposition process. In all experiments a pronounced surface holdup is observed, which increases with increasing deposition rate. For Au (Figure 3) the deposition rate and the surface holdup are substantially smaller than for Ag (Figure 4). Similar results have been found for diffusion of Cu and Ag in the polyimide PMDA-ODA,^{24,25} where the concentration in the polymer can vary by several decades depending on the deposition rate. The rate dependence was attributed to the strong tendency of the metal atoms to aggregate. This was attributed to a weak nonlocalized interaction between noble metal atoms and functional groups of the polymer^{16,38–40} and the strong metal–metal interaction, which is much higher than the polymer–polymer interaction. In addition, the nonlocalized weak interaction with the polymer gives rise to a high metal mobility on the surface.^{41,42} Therefore, most atoms form immobile clusters at the surface when deposited at high rates. At low deposition rates a large fraction of isolated atoms is able to diffuse into the bulk.^{24,25} This behavior

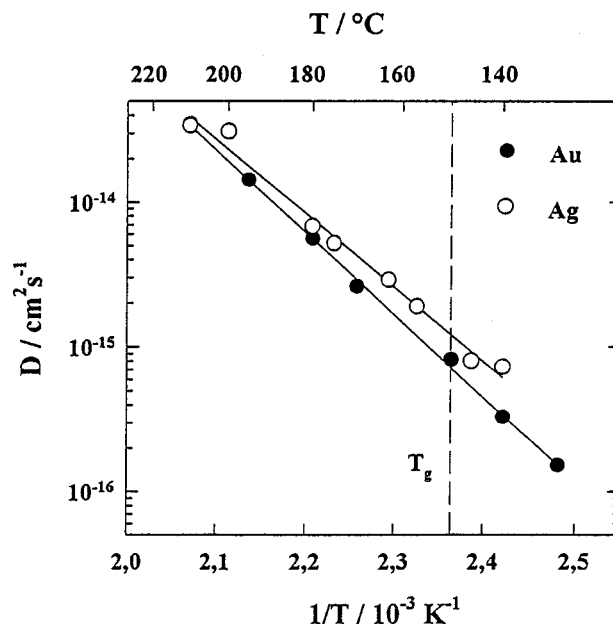


Figure 5. Arrhenius plot for diffusion of ^{110m}Ag and ^{198}Au into Bisphenol A polycarbonate. The solid lines represent the best fit for an Arrhenius law to the data. The broken line indicates the glass transition temperature measured by DSC at 20 °C/min.

is inconsistent with a well-defined solubility limit of metals in polymers. Investigations by cross-sectional transmission electron microscopy on interface formation between Ag and PMDA-ODA²⁴ and between Au and trimethylcyclohexanone polycarbonate³⁶ have confirmed these results. In this view, the linear ranges of the penetration profiles in Figures 1, 3, and 4 are attributed to diffusion of single atoms.

It should be noted that the differences in the amount of surface holdup between silver and gold and its variation with the deposition process cannot be explained by ordering of the polymer chains near the surface, which has been observed for polyimide.³⁷

Concerning the mechanism of diffusion, the question may arise whether the metal diffuses in the state of neutral atoms or charged ions. Neutral metal atoms were deposited onto the polymer. For ionization the noble metal atoms have to be oxidized and the polymer has to be reduced. Both processes involved an energy of more than 1 eV per metal ion. In XPS and infrared reflection absorption spectroscopy no charged state has been detected for silver, gold, or the polymer, even at low surface concentrations.^{8,39,40} Thus, it is obvious that the metals gold and silver diffuse as uncharged particles into the polycarbonate. Further evidence comes from the fact that the mobility of the metal even in the rubbery state of the polymer is much lower than the mobility of ions in a typical polymer electrolyte (PEO).^{4,5}

The temperature dependence of diffusion of silver and gold in Bisphenol A polycarbonate can be well described by an Arrhenius law (Figure 5). No change in slope can be observed at the glass transition temperature T_g of 150 °C determined by DSC at a rate of 20 °C/min. On the other hand, a change in the temperature dependence was detected at 138 °C for the diffusion of dye molecules in this polymer. This change was related to the glass transition. The occurrence at the lower temperature was explained in terms of the much longer time scale of diffusion measurements in comparison to DSC measurements.²⁹ Taking into account that the annealing time for metal diffusion is of the same order of magni-

Table 2. Arrhenius Data of Diffusion in Bisphenol A Polycarbonate and Kinetic Diameter for Several Gases

gas	D_0 (cm ² s ⁻¹)	activation energy (eV)	kinetic diameter (nm)
He	0.14	0.29	0.26
CO ₂	0.020	0.36	0.33
O ₂	0.015	0.33	0.346
N ₂	0.12	0.42	0.364
CH ₄	0.074	0.44	0.38

tude as for dye diffusion and that there is only one measurement of Au diffusion in BPA below 138 °C, no reliable conclusions can be drawn on the temperature dependence at and below the glass transition. However, the glass transition does not seem to influence the diffusion behavior. We note in passing that, due to the temperature treatment prior to the evaporation process and the long annealing times in the diffusion experiments at low temperatures, an effect of physical aging near T_g on the diffusion of metals can be excluded.

Other models for diffusion in polymers and disordered media,^{43–47} which predict a nonlinear Arrhenius plot, do not provide a good description of the data in Figure 5 with reasonable values of the adjustable parameters.

The small diffusion coefficients for Ag and Au diffusion in Bisphenol A polycarbonate are in accord with the small diffusivities for noble metal diffusion in polyimides.^{22–25} By contrast, the diffusivities of several gases in Bisphenol A polycarbonate,³² which were measured over a wide temperature range, are higher by several orders of magnitudes, and the activation energies, listed in Table 2, are considerably lower than those of metals. The small differences in the activation energies for these gases are interpreted within the model of Meares⁴⁸ in terms of the different kinetic diameters of the diffusing molecules. Since the kinetic diameter is not known for noble metals, it can only be estimated from the atomic radius of these elements, which is 0.29 nm for both Au and Ag. However, the atomic radius is determined from the lattice parameter in the solid state and does not necessarily reflect the diameter of a free atom. Better values would be the van der Waal's radii of these elements, but the only data available are for mercury,⁴⁹ which follows gold in the periodic table. For this element the atomic and van der Waal's radius differ only slightly. Therefore, for silver and gold a diameter of about 0.3 nm can be assumed which is comparable to the diameter of the gases in Table 2. Following the model of Meares⁴⁸ the activation energy for diffusion of gold and silver should be much lower and similar to the activation energies for gas diffusion.³² On the other hand, one might consider a much higher kinetic diameter for the metal atoms. By extrapolating the dependence of the activation energy on the kinetic diameter, which is known for gas diffusion in various polycarbonates,³² a kinetic diameter in the range of 0.5–0.7 nm is obtained for gold and silver. This value is about twice the value of the atomic diameter and hence not realistic. Completely unrealistic hard sphere diameters are also obtained by modeling metal diffusion in the polymer above T_g in the terms of the Stokes–Einstein relationship as viscous flow.

In order to compare metal diffusion with the diffusion of some larger dye molecules²⁹ the diffusion coefficients for metals and dye molecules are plotted in Figure 6 as a function of temperature. In addition, the hypothetical self-diffusion coefficient for the segment mobility of the polymer matrix is shown. The strong temperature

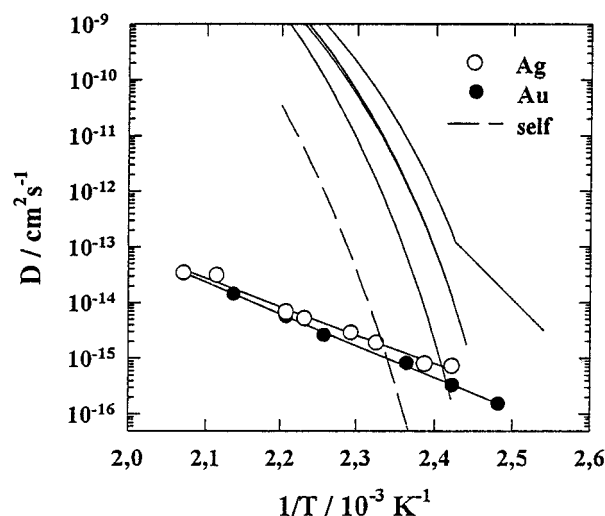


Figure 6. Comparison of diffusion of different dye molecules (after ref 29) and the metals Ag and Au in Bisphenol A polycarbonate. The dye molecules are from top to bottom: TTI; ONS-N; ONS-B; ONS-A. The dashed line represents the hypothetical self-diffusion coefficient $D_s = kT/\Lambda_0$ of the polycarbonate matrix, where Λ_0 is the monomer friction coefficient (ref 29 and therein).

dependence of the dye diffusivities and the nonlinear Arrhenius plot are well described by the free volume theory. The differences in the diffusivities reflect the slightly different coupling of the molecules of different sizes and flexibility to the polymer mobility.²⁹

It is very surprising that near the glass transition temperature the diffusivities of metal atoms, which have a much smaller size, are in the range of the diffusion coefficients of dye tracers in this polymer,²⁹ but that with increasing temperature the metal mobility does not increase like the mobility of the dye tracers does. At temperatures of about 200 °C, the metal diffusivity is lower by orders of magnitude than the diffusivities of dye tracers and also lower than the diffusivities of polymer segment diffusivity. Metal diffusion clearly follows an Arrhenius law with a much lower activation energy than the effective activation energies for dye diffusion in this polymer, which follows the Vogel–Fulcher–Tammann relation. Diffusion of silver and gold seems to be decoupled from the long-range self-diffusion of the polymer, the so-called α -process. These results are remarkable, since they show that even at high temperatures polymer self-diffusion apparently does not induce diffusion of the metal atoms, although it does so for the dye molecules larger in size and similar in weight.²⁹ The diffusion process for metal atoms seems to be blocked.

One might be tempted to attribute the slow metal diffusion and the aforementioned large kinetic diameters to diffusion of metal clusters. However, this notion is in conflict with the complete decoupling of metal diffusion from polymer dynamics, since even the much faster dye molecules exhibit a marked coupling (Figure 6).

A simple reversible bonding of metal atoms to one polymer chain, would drastically reduce the metal mobility. The diffusivity would be determined by the thermally activated process of breaking this bond and of overcoming the jumping barrier, as long as the mobility of the whole polymer chain is negligible. This is obviously true for low temperatures. However, at high temperatures the chain itself becomes mobile, and diffusion of metal atoms should be influenced by the chain diffusion.

The chain diffusivity D_C can be estimated from the segment mobility D_S and the length N of the polymer chain, $D_C = D_S N^{-\lambda}$. With an average chain length of $N = 57$ for our polymer and $\lambda = 2$, according to the model of reptation,⁵¹ the estimated diffusion coefficient for the polymer chain is in the range of $10^{-14} \text{ cm}^2 \text{ s}^{-1}$ at high temperatures and exceeds the diffusivity for the metal atoms (see Figure 6). However, the chain diffusivity D_C exhibits the temperature dependence of D_S (see Figure 6), which is entirely different from that of Ag and Au diffusion. This decoupling of metal–atom and polymer–chain diffusion suggests that the presence of the metal atoms strongly affects the local polymer dynamics.

Since a metal atom is small compared to a monomer unit, no significant geometrical obstruction of the movement of the whole chain is expected. A major reduction of the mobility of the whole chain due to the additional mass of the metal atom is not expected either; otherwise a much larger difference between diffusion of Au and Ag should be visible. In a model that is based on metal–polymer binding, diffusion of metal atoms is determined by the frequency of jumps between two neighboring chains. At low temperatures this jump process is faster than the segment mobility of the polymer chain. Therefore, the jump length is determined by the distance between two chains. However, at high temperatures, where the segment diffusivity exceeds the diffusivity of the metal atoms, a metal atom can move together with a segment of the polymer chain before it performs a jump to the next bonding site. Hence, the effective jump distance increases. This should lead to a strong increase of the diffusivity at higher temperatures and to a curvature in the Arrhenius plot. Since there is no deviation from a linear Arrhenius law, an explanation different from binding of a metal atom to one polymer chain is suggested.

The Arrhenius-like temperature dependence can be explained by molecular theories^{1–3} which were developed to describe the diffusion of gas molecules in polymers. Alternatively, an expression for thermally activated bond breaking can be incorporated into free-volume theories.^{26,27} Since the mobility of gas molecules is much higher than that of metal atoms, the lower diffusivity and higher activation energy have to be explained. In the molecular theories of DiBenedetto and Paul^{52,53} and of Pace and Dwyer^{54,55} the diffusing atom is situated between four locally parallel polymer chains. For a diffusion jump, energy has to be absorbed in a region near this atom to separate the chains and to open the diffusion path. In the case of an attractive interaction between the metal atom and one or more polymer chains, additional energy has to be absorbed for breaking the bonds. If the metal atom interacts with more than one chain, these bonds will act as local and temporary cross-links and thus reduce the mobility of the polymer chains involved. This could explain the reduced mobility of the metal atoms in comparison to the undecorated polymer segments. Within this framework the activation energy for diffusion consists of the contribution for opening the diffusion path and a contribution to overcome the binding between the metal and several polymer chains.

Even though gold and silver are noble metals, XPS measurements show a weak interaction between silver and the carbonyl oxygen of a polymer.^{8,39} Further evidence for an interaction is that both gold and silver significantly catalyze the cross-linking of a polymer, although this effect is less pronounced than for the more

reactive metals Fe and Ni.⁵⁶ The metal–polymer interaction could have the character of a van der Waals binding and could be a dipole/induced dipole coupling.

In the molecular theories for gas diffusion^{48,52–55} the activation energy for the opening of the diffusion path depends on the size of the diffusing atom. Since silver and gold atoms have the same size the contribution for separating the polymer chains should be the same for both. This opening process is coupled to the β -relaxation of the polymer, which is a thermally activated process with an activation energy of 0.56 eV for Bisphenol A polycarbonate.⁵⁷ With the additional contribution for breaking weak van der Waals-like bonds, the activation energy of about 1 eV for diffusion of silver and gold seems to be quite plausible.

Further evidence for this model of an additional interaction between the metal atom and several polymer chains can be obtained from the D_0 value for diffusion. The preexponential factor is given by

$$D_0 = \alpha a^2 \nu \exp(S/k)$$

where a is the jump distance, regardless of whether the jump occurs directly from one binding site to another or involves movement with the chain, ν is the vibrational frequency, α is a factor which depends on the geometrical structure and on the correlation between successive jumps, S is the entropy of diffusion, and k is the Boltzmann constant.³⁵ In amorphous systems these are averaged quantities. The D_0 values for metal diffusion are only slightly smaller than for gas diffusion. While the jump distance a and the factor α should be nearly the same for diffusion of gases and metals, this is not to be expected for the vibrational frequency ν and the entropy S . For gas diffusion, which is measured in the glassy state, the polymer structure can be assumed as rigid and stable on the time scale of a diffusion jump of a gas molecule. However, for metal diffusion in the rubbery state the polymer structure can no longer be assumed to be stable on the time scale of a diffusion jump, judging from the very low diffusivities of metals. The potential barriers for a diffusion jump should relax due to the mobility of the polymer chains. Therefore, it is to be expected that the vibrational frequency and entropy, and thus the D_0 value, are different for slow diffusion in the rubbery and fast diffusion in the glassy state. By contrast, the nearly identical D_0 prefactors for metal and gas diffusion indicate that the local mobility of the polymer chains in the rubbery state is drastically reduced near metal atoms. This behavior can be explained in our model in terms of a binding of a metal atom to several chains. This temporal cross-linking reduces the local mobility of the polymer chains. Nevertheless, while our investigations provide strong evidence for a substantial interaction between Au and Ag atoms with the polymer, we cannot completely exclude from our data that the strong reduction in local mobility of the polymer chain through a metal atom is already caused by a binding to only one chain. For polymer electrolytes computer simulations have shown that Li^+ ions reduce the mobility of polymer chains in poly(ethylene oxide) drastically.⁵⁸

5. Conclusions

Diffusion of gold and silver in Bisphenol A polycarbonate is slower by about 6–8 orders of magnitude than diffusion of simple gases in this polymer. A surface

holdup of these metals, depending on the evaporation process, was observed. It reflects the tendency of the metals to form agglomerates at or near the surface due to their high cohesive energy. The temperature dependence of metal diffusion is well described by an Arrhenius law with preexponential factors being similar to those for gas diffusion but with much higher activation energies. Based on molecular theories for gas diffusion and a comparison with the segment mobility of the polymer matrix the experimental data can be explained in terms of interaction between metal atoms and polymer chains. In particular, the decoupling of metal diffusion from the polymer dynamics is interpreted as an indication of an interaction of a metal atom with several polymer chains and a resulting temporary cross-linking which strongly reduces the local mobility of the polymer chains.

Acknowledgment. The authors would like to thank A. Thran and T. Strunskus for discussions and critical reading the manuscript. The radiotracer measurements were performed in the group of Th. Hehenkamp at the Institut für Metallphysik of the University of Göttingen. The neutron activation of the radioactive tracers was carried out by GKSS Geesthacht, Germany. Financial support of this work by Volkswagen-Stiftung is gratefully acknowledged.

References and Notes

- (1) Crank, J.; Park, G. S. *Diffusion in Polymers*; Academic Press: London, 1968.
- (2) Frisch, H. L.; Stern, S. A. *CRC Crit. Rev. Solid State Mater. Sci.* **1983**, *11*, 123.
- (3) Vieth, R. W. *Diffusion in and through Polymers*; Hanser: Munich, 1991.
- (4) Gray, F. M. *Solid Polymer Electrolytes*; VCH Publishers: Weinheim, 1991.
- (5) Ratner, M. A.; Shriver, D. F. *MRS Bull.* **1989**, *14* (9), 39.
- (6) Clabes, J. G. *J. Vac. Sci. Technol. A* **1988**, *6*, 2887.
- (7) Clabes, J. G.; Goldberg, M. J.; Viehbeck, A.; Kovac, C. A. *J. Vac. Sci. Technol. A* **1988**, *6*, 985.
- (8) Strunskus, T. Ph.D. thesis, University of Heidelberg, 1993.
- (9) Reiter, G.; Hüttenbach, S.; Foster, M.; Stamm, M. *Macromolecules* **1991**, *24*, 1179.
- (10) Kunz, M.; Shull, K. *Polymer* **1993**, *34*, 2427.
- (11) Kirkaldy, J. S.; Young, D. J. *Diffusion in the Condensed State*; The Institute of Metals: London, 1987.
- (12) Tummala, R. R.; Pmaszewski, E. J. *Microelectronics Packaging Handbook*; Van Nostrand Reinhold: New York, 1989.
- (13) Larsen, R. J. *Res. Dev.* **1980**, *24*, 268.
- (14) Mittal, E. L.; Susko, J. R., Eds. *Metallized Plastics 1, 2, 3*; Plenum Press: New York, 1989, 1990, 1992.
- (15) Lin, O. C. C.; Liu, J. M. *MRL Bull. Res. Dev.* **1989**, *3*, 1.
- (16) Ho, P. S.; Haight, R.; White, R. C.; Silverman, B. D.; Faupel, F. In *Fundamentals of Adhesion*; Lee, L. H., Ed.; Plenum Publishing Co.: New York, 1991.
- (17) Hahn, P. O.; Rubloff, G. W.; Ho, P. S. *J. Vac. Sci. Technol. A* **1984**, *2*, 756.
- (18) Paik, K. W.; Ruoff, A. L. *Mater. Res. Soc. Symp. Proc.* **1989**, *153*, 143.
- (19) Shanker, K.; MacDonald, J. R. *J. Vac. Sci. Technol. A* **1987**, *5*, 2894.
- (20) Tromp, R. M.; LeGoues, F.; Ho, P. S. *J. Vac. Sci. Technol. A* **1985**, *3*, 782.
- (21) Hahn, P. O.; Rubloff, G. W.; Bartha, J. W.; LeGoues, F.; Tromp, R.; Ho, P. S. *Mater. Res. Soc. Symp. Proc.* **1985**, *40*, 251.
- (22) Faupel, F.; Gupta, D.; Silverman, B. D.; Ho, P. S. *Appl. Phys. Lett.* **1989**, *55*, 357.
- (23) Faupel, F. *Adv. Mater.* **1990**, *2*, 266.
- (24) Faupel, F. *Phys. Stat. Solids (a)* **1992**, *134*, 9.
- (25) Faupel, F. In *Polymer-Solid Interfaces*; Pireaux, J. J., Bertrand, P., Brédas, J. L., Eds.; Institute of Physical Publishing: Bristol and Philadelphia, 1992.
- (26) Vrentas, J. S.; Duda, J. L. *J. Polym. Sci.* **1977**, *15*, 403.
- (27) Vrentas, J. S.; Duda, J. L. *J. Appl. Polym. Sci.* **1978**, *22*, 2325.
- (28) Cohen, M. H.; Turnbull, D. *J. Chem. Phys.* **1959**, *31*, 1164.
- (29) Ehrlich, D.; Sillescu, H. *Macromolecules* **1990**, *13*, 1600.
- (30) Mercier, J. P.; Aklonis, J. J.; Litt, M.; Tobolsky, A. V. *J. Appl. Polym. Sci.* **1965**, *9*, 447.
- (31) Muruganandam, N.; Koros, W. J.; Paul, D. R. *J. Polym. Sci., Polym. Phys. Ed.* **1987**, *25*, 1999.
- (32) Costello, L. M.; Koros, W. J. *J. Polym. Sci., Polym. Phys. Ed.* **1994**, *32*, 701.
- (33) Faupel, F.; Hüppe, P. W.; Rätzke, K.; Willecke, R.; Hehenkamp, Th. *J. Vac. Sci. Technol. A* **1992**, *10*, 92.
- (34) Reader, P. D.; Kaufman, H. R. *J. Vac. Sci. Technol.* **1975**, *12*, 1344.
- (35) Philibert, J. *Atom movements diffusion and mass transport in solids*; Monographies de Physique, les Editions de Physique; Cedex, France, 1991.
- (36) Faupel, F.; Willecke, R.; Thran, A.; Bechtolsheim, C. v.; Kiene, M.; Strunskus, T. In *Proceedings of the International Conference on Adhesion Science Technology*, Amsterdam, 1995; Ooij, W. J. van, Groesbeek, J. R. F. Th., Eds.; International Science Publishers (in press).
- (37) Factor, B. J.; Russel, T. P.; Toney, M. F. *Phys. Rev. Lett.* **1991**, *66*, 1181.
- (38) Bartha, J. W.; Hahn, P. O.; LeGoues, F.; Ho, P. S. *J. Vac. Sci. Technol. A* **1985**, *3*, 1390.
- (39) Gerenser, L. J. *J. Vac. Sci. Technol. A* **1990**, *8*, 3682.
- (40) Strunskus, T.; Hahn, C.; Frankel, D.; Grunze, M. *J. Vac. Sci. Technol. A* **1991**, *9*, 1272.
- (41) Kunz, M. S.; Shull, K. R.; Kellock, A. J. *J. Appl. Phys.* **1992**, *72*, 4458.
- (42) Wetzel, J. T.; Smith, D. A.; Appleby-Mougham, G. *Mater. Res. Soc. Symp. Proc.* **1985**, *40*, 271.
- (43) Haus, J. W.; Kehr, K. W. *Phys. Rep.* **1987**, *150*, 263.
- (44) Kirchheim, R. *J. Non-Cryst. Solids* **1983**, *55*, 243.
- (45) Kirchheim, R.; Stolz, U. *J. Non-Cryst. Solids* **1985**, *70*, 323.
- (46) Kronmüller, H.; Frank, W. *Radiat. Eff. Def. Solids* **1989**, *108*, 81.
- (47) Bäessler, H. *Phys. Rev. Lett.* **1987**, *58*, 767.
- (48) Meares, P. *J. Am. Chem. Soc.* **1954**, *76*, 1947.
- (49) *Handbook of Chemistry and Physics*, 62nd ed.; CRC Press: Boca Raton, FL, 1981.
- (50) Ferry, J. D. *Viscoelastic Properties of Polymers*, 3rd ed.; Wiley: New York, 1980.
- (51) de Gennes, P.-G. *Scaling Concepts in Polymer Physics*; Cornell University Press: Ithaca, NY, 1979.
- (52) DiBenedetto, A. T. *J. Polym. Sci. A* **1963**, *1*, 3459, 3477.
- (53) DiBenedetto, A. T.; Paul, D. R. *J. Polym. Sci. A* **1964**, *2*, 1001.
- (54) Pace, R. J.; Datyner, A. *J. Polym. Sci., Polym. Eng. Sci.* **1979**, *20*, 51.
- (55) Pace, R. J.; Datyner, A. *J. Polym. Sci., Polym. Phys. Ed.* **1979**, *17*, 437, 453, 465, 1675.
- (56) Vogel, S. L.; Schonhorn, H. *J. Appl. Polym. Sci.* **1979**, *23*, 495.
- (57) Katana, G.; Kremer, F.; Fischer, E. W.; Plaetschke, R. *Macromolecules* **1993**, *26*, 3075.
- (58) Müller-Plathe, F.; van Gunsteren, W. F. *J. Chem. Phys.* **1995**, *103*, 4745.

MA951457+